



Journal of Coordination Chemistry

Publication details, including instructions for authors and subscription information:

<http://www.tandfonline.com/loi/gcoo20>

Synthesis, characterization, and antibacterial evaluation of copper(II) complexes supported by phenylacetic acid derivatives, and diamine ligands

Wei-Ming Zhang^{ab}, Ming-Hui Li^{ab}, Juan Sun^{ab}, Peng-Cheng Lv^{ab} & Hai-Liang Zhu^{ab}

^a Nanjing Institute for the Comprehensive Utilization of Wild Plant, Nanjing, PR China

^b State Key Laboratory of Pharmaceutical Biotechnology, Nanjing University, Nanjing, PR China

Accepted author version posted online: 24 Oct 2014. Published online: 04 Nov 2014.



CrossMark

[Click for updates](#)

To cite this article: Wei-Ming Zhang, Ming-Hui Li, Juan Sun, Peng-Cheng Lv & Hai-Liang Zhu (2014) Synthesis, characterization, and antibacterial evaluation of copper(II) complexes supported by phenylacetic acid derivatives, and diamine ligands, *Journal of Coordination Chemistry*, 67:21, 3519-3531, DOI: [10.1080/00958972.2014.976563](https://doi.org/10.1080/00958972.2014.976563)

To link to this article: <http://dx.doi.org/10.1080/00958972.2014.976563>

PLEASE SCROLL DOWN FOR ARTICLE

Taylor & Francis makes every effort to ensure the accuracy of all the information (the "Content") contained in the publications on our platform. However, Taylor & Francis, our agents, and our licensors make no representations or warranties whatsoever as to the accuracy, completeness, or suitability for any purpose of the Content. Any opinions and views expressed in this publication are the opinions and views of the authors, and are not the views of or endorsed by Taylor & Francis. The accuracy of the Content should not be relied upon and should be independently verified with primary sources of information. Taylor and Francis shall not be liable for any losses, actions, claims, proceedings, demands, costs, expenses, damages, and other liabilities whatsoever or howsoever caused arising directly or indirectly in connection with, in relation to or arising out of the use of the Content.

This article may be used for research, teaching, and private study purposes. Any substantial or systematic reproduction, redistribution, reselling, loan, sub-licensing, systematic supply, or distribution in any form to anyone is expressly forbidden. Terms &

Conditions of access and use can be found at <http://www.tandfonline.com/page/terms-and-conditions>

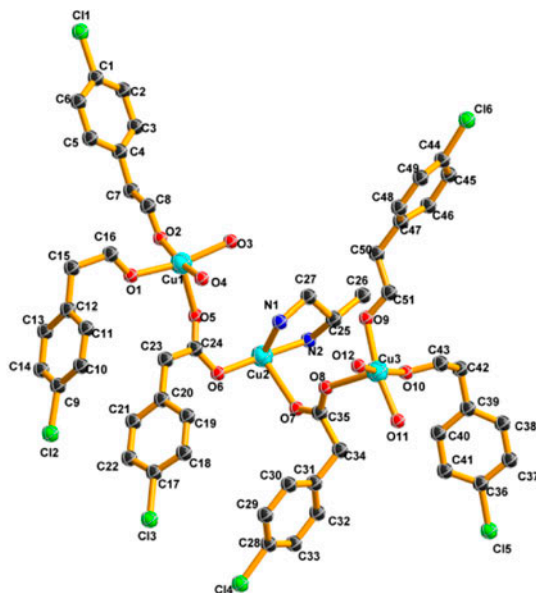
Synthesis, characterization, and antibacterial evaluation of copper(II) complexes supported by phenylacetic acid derivatives, and diamine ligands

WEI-MING ZHANG^{†‡}, MING-HUI LI^{†‡}, JUAN SUN^{†‡}, PENG-CHENG LV^{*†‡} and HAI-LIANG ZHU^{†‡}

[†]Nanjing Institute for the Comprehensive Utilization of Wild Plant, Nanjing, PR China

[‡]State Key Laboratory of Pharmaceutical Biotechnology, Nanjing University, Nanjing, PR China

(Received 1 July 2014; accepted 18 September 2014)



Four copper(II) complexes were synthesized and their structures were determined by elemental analysis and single crystal X-ray diffraction analysis. Some of them show good antibacterial activity.

Four mixed-ligand complexes, $[\text{Cu}_3(\text{cpa})_6(\text{pda})_1]$ (**1**) (cpa = 4-chlorophenylacetic acid, pda = 1,2-diaminopropane), $[\text{Cu}_3(\text{fpa})_6(\text{tn})_1]$ (**2**) (fpa = 4-fluorophenylacetic acid, tn = 1,3-diaminopropane), $[\text{Cu}_3(\text{cpa})_6(\text{en})_1]$ (**3**) (cpa = 4-chlorophenylacetic acid, en = ethylenediamine), and $[\text{Cu}_3(\text{fpa})_6(\text{pda})_1]$ (**4**) (fpa = 4-fluorophenylacetic acid, pda = 1,2-diaminopropane), were synthesized by reacting 4-chlorophenylacetic acid or 4-fluorophenylacetic acid, the diamines, and metal salts. Their structures

*Corresponding author. Email: pcvlv@nju.edu.cn

[†]These two authors contributed equally to this article.

were determined by elemental analysis and single-crystal X-ray diffraction analysis. The antimicrobial activities for the metal complexes were evaluated against *Escherichia coli*, *Pseudomonas putida*, *Bacillus subtilis*, and *Bacillus cereus*. The antimicrobial results indicated that the four synthesized complexes displayed good inhibitory activity against *E. coli* and *B. subtilis*, and could be promising antibacterial agents.

Keywords: Phenylacetic acid derivatives; Copper(II) complexes; Single-crystal X-ray analysis; Antibacterial activity

1. Introduction

Phenylacetic acid is used in some perfumes, possessing a honey-like odor. It is used in penicillin production, and also in plastic, textile, paper, insect repellent, pesticide, and cosmetic industries [1]. Phenylacetic acid and its derivatives have attracted much interest for their biological activities. Phenylacetic acid is an active auxin molecule, a type of plant hormone, which plays an essential role in coordination of many growth and behavioral processes in the plant life cycle [2, 3]. They also had antibacterial activity against micro-organisms such as *Escherichia coli* and *Bacillus subtilis* [4, 5]. Halogenation of pharmacologically active compounds has been a common method to increase their metabolic stability and lipophilicity, which could lead to increased binding affinity to the receptor, channel, transporter, or other protein target [6]. Transition metals exhibit different biological activities [7]. The antibacterial effect of certain drugs could be enhanced when chelating to a metal [8]. For example, copper complexes have excellent antibacterial activity, making them alternative antibacterial therapeutic agents [9, 10].

Here we synthesized four mixed-ligand metal complexes, $[\text{Cu}_3(\text{cpa})_6(\text{pda})_1]$ (**1**), $[\text{Cu}_3(\text{fpa})(\text{tn})_1]$ (**2**), $[\text{Cu}_3(\text{cpa})_6(\text{en})_1]$ (**3**), and $[(\text{Cu}_3(\text{fpa})_6(\text{pda})_1)]$ (**4**), using halogenated phenylacetic acids as starting materials. Their structures were determined by elemental analysis and single-crystal X-ray diffraction analysis. Their antimicrobial activities were evaluated against four different bacteria, *E. coli*, *Pseudomonas putida*, *B. subtilis*, and *Bacillus cereus*. The results suggest that some of them exhibit promising antimicrobial activity.

2. Experimental

2.1. General

All reagents, unless otherwise stated, were purchased as AR grade. Copper(II) perchlorate hexahydrate was dried under vacuum prior to use. All other reagents were used as received. Elemental analyses were conducted on a Perkin-Elmer 240C elemental analyzer, and their structures were determined by single-crystal X-ray diffraction analysis.

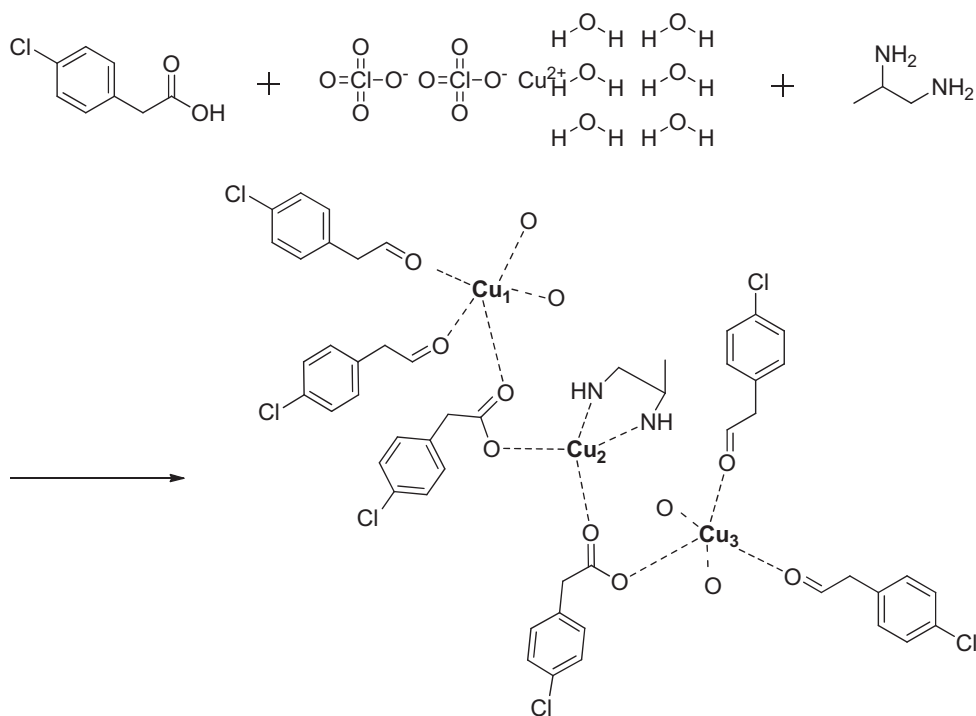
2.2. Synthesis of 1–4

The synthesis of **1–4** was performed according to the literature procedures [11] with modification. For **1**, 4-chlorophenylacetic acid (1 mM, 0.171 g) and copper(II) perchlorate hexahydrate (0.5 mM, 0.185 g) were dissolved in concentrated ammonium solution (10 mL) and the mixture was stirred for 15 min until a clear solution was obtained. Then, 1,2-propanedi-

amine (0.5 mM, 0.037 g) was added to the above-mentioned solution. The mixture was stirred at room temperature for 20 min to give a clear blue solution, which was filtered off. After keeping the solution in air for several days, blue-shaped crystals were formed at the bottom of the vessel. The blue crystals were collected by filtration and washed with ethanol three times and then air-dried. Yield: 0.128 g (32.5%). Compounds **2–4** were synthesized using the same method as for **1**. Their yields are 0.102 g (27%), 0.135 g (35%), and 0.165 g (44%), respectively. The synthetic route for **1** is shown in scheme 1.

2.3. X-ray crystallographic analysis

Single-crystal X-ray diffraction data were collected on a Bruker D-8 Venture diffractometer at room temperature (293 K). The X-ray generator was operated at 50 kV and 35 mA using Mo K α radiation ($\lambda = 0.71073 \text{ \AA}$). The data were collected using the SMART software package. The data were reduced by SAINT-PLUS, an empirical absorption correction was applied using SADABS and XPREP was used to determine the space group. The crystal structure was solved by direct methods using SIR92 and refined by full-matrix least-squares using SHELXL97 [12, 13]. All non-hydrogen atoms were refined anisotropically and hydrogens were refined in the riding mode on their carrier atoms wherever applicable. Experimental details for X-ray data collection of **1–4** are presented in table 1. Molecular structures and the atomic numbering scheme of **1–4** are shown in figures 1–4, respectively.



Scheme 1. The synthetic route for **1**.

Table 1. Crystallographic data and details of diffraction experiments for 1–4.

	1	2	3	4
Empirical formula	$C_{51}H_{46}Cl_6Cu_3N_2O_{12}$	$C_{51}H_{46}Cu_3F_6N_2O_{12}$	$C_{50}H_{44}Cl_6Cu_3N_2O_{12}$	$C_{51}H_{46}Cu_3F_6N_2O_{12}$
Color	Blue	Blue	Blue	Blue
Formula weight	1282.25	1183.55	1268.22	1183.55
Temperature (K)	273	273	273	273
Crystal system	Triclinic	Triclinic	Triclinic	Triclinic
Space group	<i>P</i> -1	<i>P</i> -1	<i>P</i> -1	<i>P</i> -1
Unit cell dimensions (\AA , $^\circ$)				
<i>a</i> (\AA)	13.6696(17)	13.6372(5)	13.6798(10)	13.4885(6)
<i>b</i> (\AA)	14.9622(19)	14.1511(6)	14.6588(10)	14.1962(7)
<i>c</i> (\AA)	15.0312(19)	15.2196(7)	14.9467(10)	15.1911(7)
α ($^\circ$)	90.729(4)	65.792(1)	89.611(2)	66.960(1)
β ($^\circ$)	116.797(3)	72.843(1)	83.643(2)	71.730(1)
γ ($^\circ$)	95.198(3)	87.249(1)	64.139(2)	86.267(2)
<i>V</i> (\AA^3)	2727.9(6)	2550.63(19)	2677.6(3)	2536.4(2)
<i>Z</i>	2	2	2	2
<i>F</i> (0 0 0)	1302	1206	1286	1286
Calculated density (g cm^{-3})	1.561	1.514	1.573	1.573
Absorption coefficient (mm^{-1})	1.514	1.325	1.542	1.542
Temperature (K)	273	273	273	273
Reflections collected	10,444	9748	10,168	9684
Independent reflection	10,243	9733	10,123	9659
Refined parameters	668	667	658	668
θ Range for data collection ($^\circ$)	2.0–25.7	2.1–25.7	2.0–25.7	2.1–25.7
Final <i>R</i> indices [<i>I</i> > 2 σ (<i>I</i>)]	<i>R</i> ₁ = 0.080, <i>wR</i> ₂ = 0.202	<i>R</i> ₁ = 0.046, <i>wR</i> ₂ = 0.117	<i>R</i> ₁ = 0.059, <i>wR</i> ₂ = 0.159	<i>R</i> ₁ = 0.043, <i>wR</i> ₂ = 0.115
<i>R</i> indices (all data)	<i>R</i> ₁ = 0.0802, <i>wR</i> ₂ = 0.2015	<i>R</i> ₁ = 0.0462, <i>wR</i> ₂ = 0.1166	<i>R</i> ₁ = 0.0462, <i>wR</i> ₂ = 0.1166	<i>R</i> ₁ = 0.0432, <i>wR</i> ₂ = 0.1151
Goodness-of-fit	1.018	1.04	1.01	1.10
Largest diff. peak/hole (e \AA^{-3})	0.98/−1.09	0.62/−0.59	0.95/−0.50	0.88/−0.68

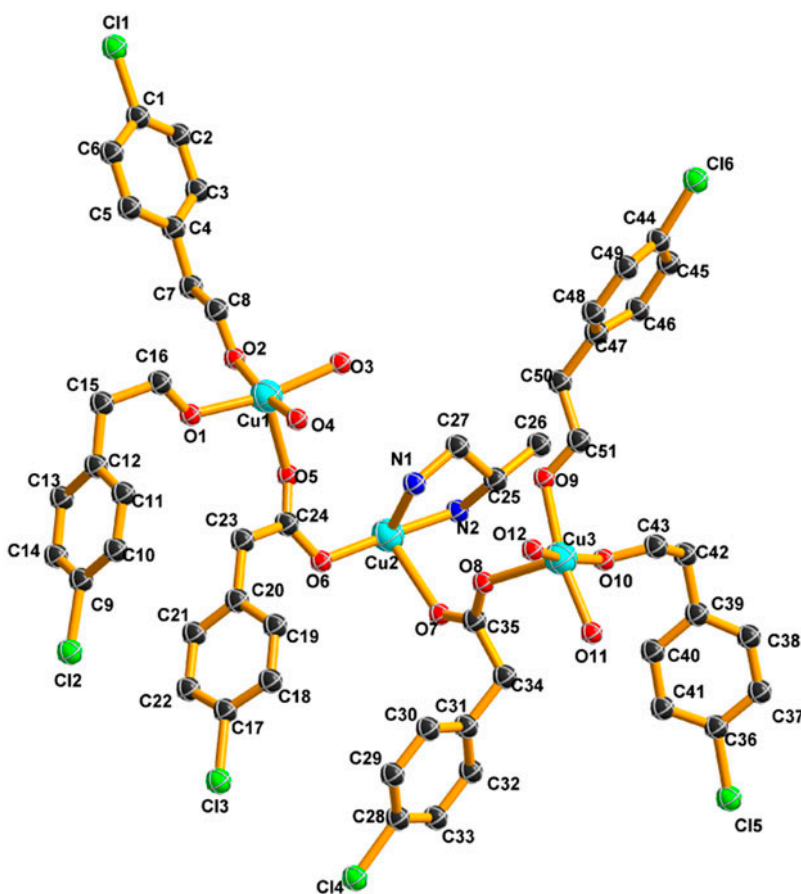


Figure 1. ORTEP view of $[\text{Cu}_3(\text{cpa})_6(\text{pda})]$ (1) with atom labeling scheme. Thermal ellipsoids are shown at 30% probability. Hydrogens have been omitted for clarity.

2.4. Antimicrobial activity

The antibacterial activities of the synthesized compounds were performed according to the literature procedures [14] with modification. The antibacterial activities of the synthesized compounds were tested against *E. coli*, *P. putida*, *B. subtilis*, and *B. cereus* using MH medium (Mueller-Hinton medium: case in hydrolysate 17.5 g, soluble starch 1.5 g, beef extract 2.0 g, distilled water 1000 mL). The inhibition (%) of the growth of different bacteria by the test complexes were determined by a colorimetric method using the dye MTT (3-(4,5-dimethylthiazol-2-yl)-2,5-diphenyl tetrazolium bromide) [15]. A stock solution of the synthesized compound ($50 \mu\text{g mL}^{-1}$) in DMSO was prepared and graded quantities of the test compounds were incorporated in specified quantity of sterilized MH. A specified quantity of the medium containing the test compound was poured into microtitration plates. Suspension of the microorganism was prepared to contain approximately 10^5 cfu mL^{-1} and applied to microtitration plates with serially diluted compounds in DMSO to be tested and incubated at 37°C for *E. coli* and *B. subtilis*, and at 30°C for *P. putida*, and *B. cereus* for 24 h. After the inhibitions (%) of the growth of different bacteria were visually determined on each of the microtitration

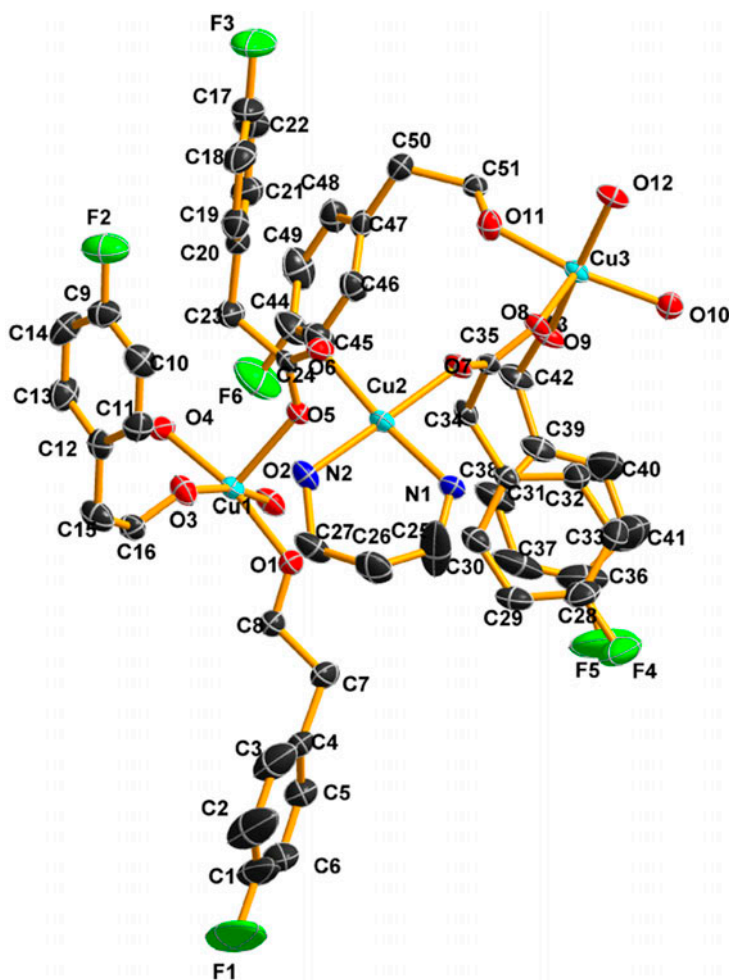


Figure 2. ORTEP view of [Cu₃(fpa)₆(tn)₁] (2) with atom labeling scheme. Thermal ellipsoids are shown at 30% probability. Hydrogens have been omitted for clarity.

plates, 50 μL of phosphate buffered saline (PBS) 0.01 mL^{-1} , pH 7.4: Na₂HPO₄·12H₂O 2.9 g, KH₂PO₄ 0.2 g, NaCl 8.0 g, KCl 0.2 g, distilled water 1000 mL] containing 2 mg mL^{-1} MTT was added to each well. Incubation was continued at room temperature for 4–5 h. The content of each well was removed and 100 μL of isopropanol containing 5% 1 mL^{-1} HCl was added to extract the dye. After 12 h of incubation at room temperature, the optical density was measured with a microplate reader at 550 nm. The inhibition (%) of the growth of different bacteria by the test complexes are presented in table 2.

3. Results and discussion

3.1. Single-crystal X-ray diffraction analysis

Single-crystal X-ray diffraction analyses revealed all four complexes were asymmetric trinuclear units although different phenylacetic acid ligands and diamine ligands were employed

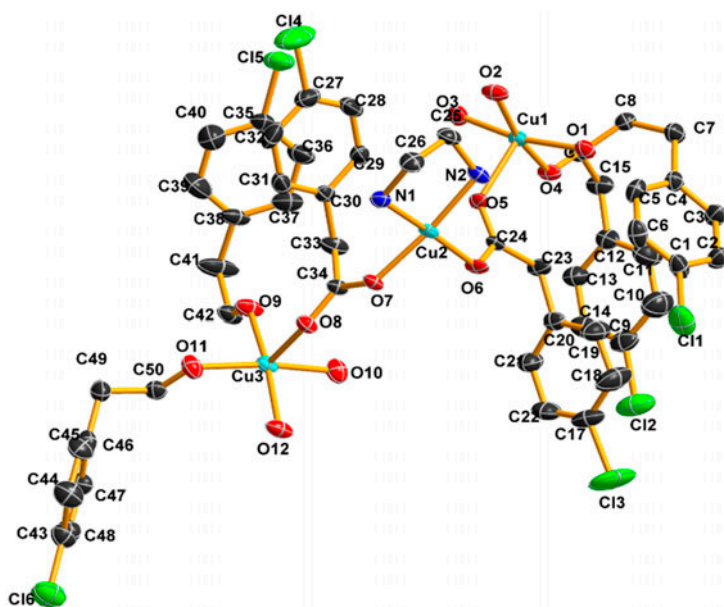


Figure 3. ORTEP view of $[\text{Cu}_3(\text{cpa})_6(\text{en})_1]$ (**3**) with atom labeling scheme. Thermal ellipsoids are shown at 30% probability. Hydrogens have been omitted for clarity.

during the synthetic procedures. Selected bond lengths and angles for **1–4** are given in table 3, and the hydrogen-bonding geometry for **1–4** are shown in table 4. In all complexes, Cu1 and Cu3 were coordinated by five oxygens from their corresponding phenylacetic acid ligands. Cu2 was coordinated by two nitrogens from the diamine ligands and two oxygens from the phenylacetic acid ligands. According to Addison and Rao [16, 17], the distortion of the square-pyramidal geometry toward trigonal bipyramidal can be described by geometrical parameter $\tau = (\beta - \alpha) / 60$, where β and α are the two largest coordination angles; $\tau = 0$ for perfect square pyramidal and 1 for trigonal bipyramidal geometry. In this case, all copper ions of all complexes adopt similar perfect square-pyramidal-based structures ($\tau = 0.5\text{--}0.7\%$).

Generally, the $\text{Cu-L}_{\text{axial}}$ bond is longer than the $\text{Cu-L}_{\text{equatorial}}$ bond in square-pyramidal complexes, while the opposite is true in trigonal-bipyramidal geometry [18]. In **1** (figure 1), $\text{Cu1-L}_{\text{apical}}$ bond length is 2.147(5) Å and $\text{Cu1-L}_{\text{basal}}$ bond length ranges from 1.9459(16) to 1.9832(19) Å. $\text{Cu3-L}_{\text{apical}}$ bond length is 2.225(5) Å and $\text{Cu3-L}_{\text{basal}}$ bond length ranges from 1.935(5) to 1.976(5) Å. The four basal atoms are very nearly coplanar with mean deviation from plane of 0.0041 Å for Cu1 and 0.0029 Å for Cu3. Cu1 and Cu3 lie out of their corresponding basal planes by 0.2011 and 0.2073 Å in the direction of their corresponding axially bonded ligands. The 1,2-propanediamine chelated with the Cu2 center resulting in the five-membered chelated ring N1–C27–C25–N2–Cu2. The five-membered chelate ring in the complex is puckered so that the torsion angle of N1–C1–C2–N2 is 50.713°. The five-membered ring has half-chair conformation with the puckering parameters [19, 20] $q_2 = 0.422(8)$ Å and $\varphi_2 = 265.8(7)^\circ$.

In **2** (figure 2), $\text{Cu1-L}_{\text{apical}}$ bond length is 2.1948(17) Å and $\text{Cu1-L}_{\text{basal}}$ bond length ranges from 1.9459(16) to 1.9832(19) Å. $\text{Cu3-L}_{\text{apical}}$ bond length is 2.1948(17) Å and $\text{Cu3-L}_{\text{basal}}$ bond length ranges from 1.9459(16) to 1.9832(19) Å. The four basal atoms are

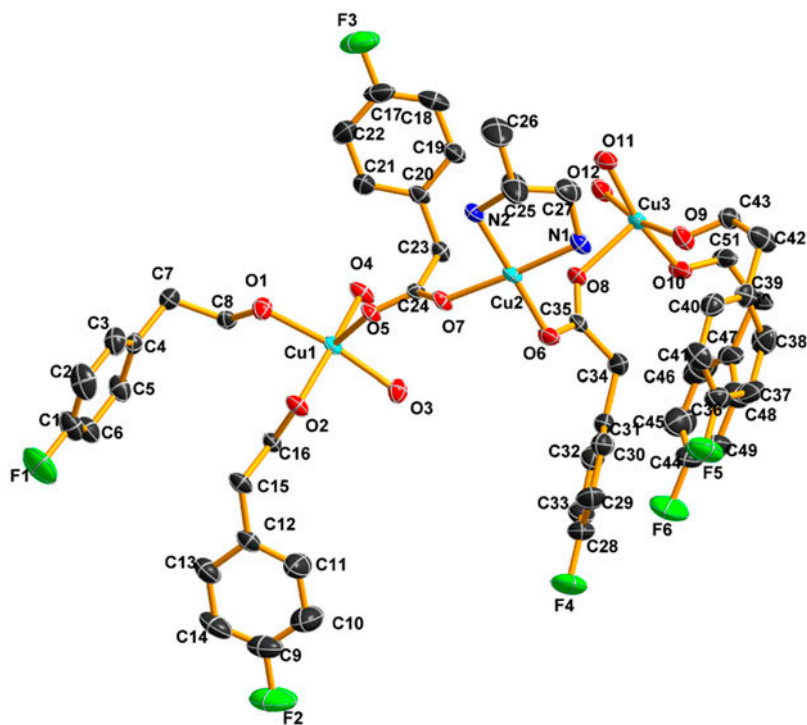


Figure 4. ORTEP view of $[\text{Cu}_3(\text{fpa})_6(\text{pda})]$ (**4**) with atom labeling scheme. Thermal ellipsoids are shown at 30% probability. Hydrogens have been omitted for clarity.

also nearly coplanar with the mean deviation from plane of 0.0002 \AA for Cu1 and 0.0001 \AA for Cu3. Cu1 and Cu3 lie out of their corresponding basal planes by 0.2005 and 0.2086 \AA in the direction of their corresponding axially bonded ligands. Cu2 is coordinated by two nitrogens from 1,3-propanediamine ligand and two oxygens from the phenylacetic acid ligands. The 1,3-propanediamine chelated with Cu2 center resulting in the six-membered chelated ring N1–C25–C26–C27–N2–Cu2. The chelate rings formed have chair conformation with the puckering parameters, $q_2 = 0.304(6) \text{ \AA}$, $\varphi_2 = 55.5(10)^\circ$, and $\varphi_3 = -0.236(5)^\circ$. The puckering parameters z_1 , z_2 , and z_3 are -0.0090 , 0.0858 , and -0.4685 \AA , respectively. The z_i values describe a distance of a carbon from a CuN1N2-plane. Thus, it seems that the chair is slightly skewed, because the z_1 and z_3 values are significantly different. The angles Cu2–N1–C25 and Cu2–N2–C27 have values $123.1(4)^\circ$ and $121.0(3)^\circ$, respectively. A plausible explanation for the deviations described above may be hydrogen-bonding interactions N1–H1B \cdots O6 and N2–H2A \cdots O8 with respect to the chelate ring.

In **3** (figure 3), Cu1– L_{apical} bond length is $2.134(3) \text{ \AA}$ and Cu1– L_{basal} bond length ranges from $1.956(4)$ to $1.964(4) \text{ \AA}$. Cu3– L_{apical} bond length is $2.212(3) \text{ \AA}$ and Cu3– L_{basal} bond length ranges from $1.955(4)$ to $1.961(3) \text{ \AA}$. The four basal atoms are very nearly coplanar with mean deviation from plane of 0.0024 \AA for Cu1 and 0.0012 \AA for Cu(3). Cu1 and Cu3 lie out of their corresponding basal planes by 0.1970 and 0.2045 \AA in the direction of their corresponding axially bonded ligands. Cu2 is coordinated by two nitrogens from the ethylenediamine and two oxygens from the phenylacetic acid ligands. The ligand ethylenediamine chelated with Cu2 to result in the five-membered chelated ring

Table 2. Inhibition (%) of the growth of different bacteria by 1–4.

Complex	Final conc. ($\mu\text{g mL}^{-1}$)	Bacteria			
		Gram-negative		Gram-positive	
		<i>P. putida</i>	<i>E. coli</i>	<i>B. cereus</i>	<i>B. subtilis</i>
1	100	–	83.91	–	43.66
	50	–	77.83	–	8.52
	25	–	73.76	–	–
	12.5	–	75.04	–	–
	100	–	82.41	–	30.07
2	50	–	75.35	–	12.66
	25	–	74.09	–	1.83
	12.5	–	70.67	–	–
	100	–	81.55	–	16.40
	50	–	79.08	–	–
3	25	–	76.10	–	–
	12.5	–	73.70	–	–
	100	–	90.50	–	22.87
	50	–	80.24	–	4.89
	25	–	–	–	–
4	12.5	–	–	–	–
	100	96.61	98.17	97.50	94.92
	50	88.77	96.70	85.29	93.89
	25	47.57	92.16	46.69	90.92
	12.5	42.92	89.93	28.57	89.85
Chloramphenicol					

N1–C26–C25–N2–Cu2. The chelate rings formed by en have half-chair conformation with the puckering parameters $q_2 = 0.429(6)$ Å and $\varphi_2 = 89.4(5)^\circ$. The mean Cu–N(amine) distance of 1.998 Å and bite angle N1–Cu2–N2 of $84.54(17)^\circ$ are close to the corresponding average values of the copper(II) complexes with ethylenediamine [21, 22]. The five-membered chelate ring in the complex is puckered so that the torsion angle of N2–C25–C2–N1 is $-51.7(6)^\circ$. The distortion may be attributable to hydrogen-bonding interactions N1–H1B \cdots O6 and N2–H2A \cdots O8 with respect to the chelate ring.

In 4 (figure 4), Cu1–L_{apical} bond length is 2.178(2) Å and Cu1–L_{basal} bond length ranges from 1.958(2) to 1.977(2) Å. Cu3–L_{apical} bond length is 2.117(2) Å and Cu3–L_{basal} bond length ranges from 1.954(3) to 1.973(2) Å. The four basal atoms are nearly coplanar with the mean deviation from plane of 0.0017 Å for Cu1 and 0.0011 Å for Cu3. Cu1 and Cu3 lie out of their corresponding basal plane by 0.2051 Å and 0.1997 Å in the direction of their corresponding axially bonded ligands. Cu2 is coordinated by two nitrogens from the 1,2-propanediamine and two oxygens from the phenylacetic acid ligands. The 1,2-propanediamine chelated with the Cu2 center to result in the five-membered chelated ring N1–C27–C25–N2–Cu2. The five-membered chelate ring in the complex is puckered so that the torsion angle of N1–C27–C25–N2 is -44.31° . The chelate ring has half-chair conformation with the puckering parameters, $q_2 = 0.349(5)$ Å and $\varphi_2 = 96.3(5)^\circ$.

Tricopper complex research is becoming more comprehensive and important. For example, three triangular trinuclear copper(II) complexes bridged by carbonate have been synthesized and structurally characterized by Huang and coworkers [23]. Carbonates originate from atmospheric CO₂ when the solutions are exposed to air for a long time. The copper(II) centers are five-coordinate trigonal bipyramidal and square pyramidal as well as six-coordinate octahedral [23]. In 2014, Mondal *et al.* reported the synthesis, characterization, and crystal structure of a heteropentanuclear Cu^{II}₃Tl^I₂ compound, which crystallizes in the monoclinic crystal system within space group C2/c. Each of the two symmetry-related

Table 3. Selected bond distances (Å) and angles (°) for 1–4.

Complex 1					
Cu1–O1	1.963(5)	O1–Cu1–O2	90.2(2)	O7–Cu2–N2	87.88(18)
Cu1–O3	1.973(6)	O1–Cu1–O3	168.1(2)	O7–Cu2–O7b	85.77(17)
Cu1–O(4)	1.964(6)	O1–Cu1–O4	89.7(2)	N1–Cu2–N2	84.5(2)
Cu1–O5	2.147(5)	O1–Cu1–O5	99.32(19)	N1–Cu2–O7b	174.3(2)
Cu2–O6	1.960(4)	O2–Cu1–O3	89.3(2)	N2–Cu2–O7b	89.7(2)
Cu2–O7	2.388(4)	O2–Cu1–O4	168.5(2)	O8–Cu3–O9	90.6(2)
Cu2–N1	1.990(6)	O2–Cu1–O5	98.3(2)	O8–Cu3–O10	90.4(2)
Cu2–O7b	1.973(5)	O3–Cu1–O4	88.5(2)	O8–Cu3–O11	101.2(2)
Cu3–O8	2.225(5)	O3–Cu1–O5	92.51(19)	O8–Cu3–O12	101.8(2)
Cu3–O9	1.964(5)	O4–Cu1–O5	93.1(2)	O9–Cu3–O10	89.8(2)
Cu3–O10	1.935(5)	O6–Cu2–O7	90.05(17)	O9–Cu3–O11	168.2(3)
Cu3–O11	1.976(5)	O6–Cu2–N1	95.1(2)	O9–Cu3–O12	88.5(2)
Cu3–O12	1.950(5)	O6–Cu2–N2	177.9(2)	O10–Cu3–O11	89.6(2)
		O6–Cu2–O7b	90.6(2)	O10–Cu3–O12	167.8(3)
		O7–Cu2–N1	94.23(19)	O11–Cu3–O12	89.5(2)
Complex 2					
Cu1–O1	1.969(2)	O1–Cu1–O2	87.48(11)	O6–Cu2–N2	90.66(11)
Cu1–O2	1.958(3)	O1–Cu1–O3	89.75(11)	O6–Cu2–O7b	86.17(9)
Cu1–O3	1.976(3)	O1–Cu1–O4	168.33(11)	O7–Cu2–N1	87.16(11)
Cu1–O4	1.973(2)	O1–Cu1–O5	93.01(10)	O7–Cu2–N2	179.03(10)
Cu1–O5	2.120(3)	O2–Cu1–O3	168.18(12)	O7–Cu2–O7b	84.23(8)
Cu2–O6	1.965(2)	O2–Cu1–O4	91.12(11)	N1–Cu2–N2	93.80(12)
Cu2–O7	1.990(2)	O2–Cu1–O5	100.93(11)	N1–Cu2–O7b	89.46(10)
Cu2–N1	1.997(3)	O3–Cu1–O4	89.29(11)	N2–Cu2–O7b	95.85(10)
Cu2–N2	1.980(3)	O3–Cu1–O5	90.69(11)	O8–Cu3–O9	98.70(9)
Cu2–O7b	2.357(2)	O4–Cu1–O5	98.63(10)	O8–Cu3–O10	102.50(9)
Cu3–O8	2.185(2)	O5–Cu2–O6	50.16(9)	O8–Cu3–O11	89.69(9)
Cu3–O9	1.963(3)	O5–Cu2–O7	96.71(8)	O8–Cu3–O12	93.53(9)
Cu3–O10	1.963(2)	O5–Cu2–N1	134.40(10)	O9–Cu3–O10	89.87(11)
Cu3–O11	1.959(2)	O5–Cu2–N2	82.56(10)	O9–Cu3–O11	89.09(11)
Cu3–O12	1.973(2)	O5–Cu2–O7b	136.14(7)	O9–Cu3–O12	167.76(10)
		O6–Cu2–O7	88.38(10)	O10–Cu3–O11	167.79(10)
		O6–Cu2–N1	174.05(12)		
Complex 3					
Cu1–O1	1.958(4)	O1–Cu1–O2	88.74(18)	O7–Cu2–N2	173.58(14)
Cu1–O2	1.964(4)	O1–Cu1–O3	168.60(14)	O7–Cu2–O7b	85.29(11)
Cu1–O3	1.956(4)	O1–Cu1–O4	89.08(16)	N1–Cu2–N2	84.54(17)
Cu1–O4	1.963(3)	O1–Cu1–O5	93.77(14)	N1–Cu2–O7b	87.99(14)
Cu1–O5	2.134(3)	O2–Cu1–O3	89.55(17)	N2–Cu2–O7b	96.60(13)
Cu2–O6	1.953(3)	O2–Cu1–O4	168.27(14)	O8–Cu3–O9	102.27(15)
Cu2–O7	1.967(3)	O2–Cu1–O5	91.72(13)	O8–Cu3–O10	88.99(15)
Cu2–N1	2.003(4)	O3–Cu1–O4	90.32(16)	O8–Cu3–O11	103.02(15)
Cu2–N2	1.992(4)	O3–Cu1–O5	97.55(14)	O8–Cu3–O12	89.62(15)
Cu2–O7b	2.374(3)	O4–Cu1–O5	99.93(13)	O9–Cu3–O10	89.57(17)
Cu3–O8	2.212(3)	O6–Cu2–O7	89.55(14)	O9–Cu3–O11	89.27(17)
Cu3–O9	1.961(3)	O6–Cu2–N1	175.22(15)	O9–Cu3–O12	168.08(19)
Cu3–O10	1.955(4)	O6–Cu2–N2	96.66(16)	O10–Cu3–O11	167.91(19)
Cu3–O11	1.957(4)	O6–Cu2–O7b	87.28(11)	O10–Cu3–O12	89.72(17)
Cu3–O12	1.957(3)	O7–Cu2–N1	89.40(15)	O11–Cu3–O12	88.94(17)
Complex 4					
Cu1–O1	1.958(2)	O1–Cu1–O2	87.23(10)	O7–Cu2–O7b	85.19(8)
Cu1–O2	1.977(2)	O1–Cu1–O3	168.06(10)	O8–Cu2–N1	81.15(9)
Cu1–O3	1.960(2)	O1–Cu1–O4	90.53(10)	O8–Cu2–N2	131.01(10)
Cu1–O4	1.965(2)	O1–Cu1–O5	102.50(9)	O8–Cu2–O7b	137.81(7)
Cu1–O5	2.178(2)	O2–Cu1–O3	90.79(10)	N1–Cu2–N2	85.69(11)
Cu2–O6	1.953(2)	O2–Cu1–O4	167.91(9)	N1–Cu2–O7b	94.49(10)
Cu2–O7	1.968(2)	O2–Cu1–O5	93.35(9)	N2–Cu2–O7b	89.95(10)

(Continued)

Cu2–O8	2.792(2)	O3–Cu1–O4	88.95(10)	O8–Cu3–O9	92.04(10)
Cu2–N1	1.989(3)	O3–Cu1–O5	89.37(9)	O8–Cu3–O10	98.01(9)
Cu2–N2	1.998(3)	O4–Cu1–O5	98.73(9)	O8–Cu3–O11	93.54(10)
Cu2–O7b	2.333(2)	O6–Cu2–O7	89.55(9)	O8–Cu3–O12	99.65(10)
Cu3–O8	2.117(2)	O6–Cu2–O8	51.43(8)	O9–Cu3–O10	90.21(11)
Cu3–O9	1.959(3)	O6–Cu2–N1	94.35(11)	O9–Cu3–O11	88.71(11)
Cu3–O10	1.967(2)	O6–Cu2–N2	177.48(11)	O9–Cu3–O12	168.06(11)
Cu3–O11	1.973(2)	O6–Cu2–O7b	87.53(9)	O10–Cu3–O11	168.43(11)
Cu3–O12	1.954(3)	O7–Cu2–O8	101.72(8)	O10–Cu3–O12	90.53(11)
		O7–Cu2–N11	76.07(10)	O11–Cu3–O12	88.18(11)
		O7–Cu2–N2	90.40(10)		

Note: Symmetry transformations used to generate equivalent atoms: **1**, O7b = 2 - x, -y, and 1 - z; **2**, O7b = 1 - x, 2 - y, and -z; **3**, O7b = -x, -y, and 1 - z; **4**, O7b = 4 - x, 1 - y, and 2 - z.

Table 4. Hydrogen-bonding geometry (Å and °) for **1–4**.

Bond	Distance (D_A, Å)	Angle (°)	Symmetry code
Complex 1			
N2–H2A···O6	3.162(6)	154	2 - x, -y, 1 - z
C6–H6···O8	3.451(11)	158	2 - x, 1 - y, 1 - z
C32–H32···O5	3.285(9)	143	2 - x, -y, 1 - z
Complex 2			
N1–H1B···O6	3.030(4)	154	1 - x, 2 - y, -z
N2–H2A···O8	3.018(4)	149	1 - x, 2 - y, -z
C22–H22···F1	3.176(9)	144	1 + x, 1 + y, -1 + z
Complex 3			
N1–H1B···O6	3.063(5)	153	-x, -y, 1 - z
N2–H2A···O8	3.106(5)	141	-x, -y, 1 - z
C5–H5···O8	3.396(7)	165	-x, -y, 1 - z
Complex 4			
N1–H1A···O5	3.016(4)	140	-x, 1 - y, 2 - z
N2–H2B···O6	3.113(4)	151	-x, 1 - y, 2 - z
C27–H27A···O2	3.244(5)	143	-x, 1 - y, 2 - z
C37–H37···F5	3.385(5)	152	-x, 1 - y, 1 - z

thallium(I) centers is located between a terminal and a common, central [Cu^{II}L] by forming bonds with four phenoxo and three ethoxy oxygens. This complex is the first example of a thallium(I) system in imino-phenolate Schiff base family [24].

3.2. Antimicrobial activity

The growth response (% inhibition) of the bacteria was measured in the presence of four synthesized complexes at several concentrations from 12.5 to 1000 µg mL⁻¹. Among the bacteria tested, the Gram-negative bacterium *E. coli* was the most susceptible strain, and almost all the synthesized complexes inhibited its growth at four concentrations except for **4** at 25 and 12.5 µg mL⁻¹.

Complexes **1–4** displayed potent activity with inhibition of 83.91, 82.41, 81.55, and 90.50% against *E. coli* at the final concentration of 100 $\mu\text{g mL}^{-1}$, respectively, which were comparable to the positive control chloramphenicol. Complexes **1–3** also exhibited significant inhibition of 75.04, 70.67, and 73.70% against *E. coli* at the final concentration of 12.5 $\mu\text{g mL}^{-1}$. Growth of *B. subtilis* was only partially inhibited by **1** (43.66% at a concentration of 100 $\mu\text{g mL}^{-1}$), **2** (30.07% at a concentration of 100 $\mu\text{g mL}^{-1}$), **3** (16.40% at a concentration of 100 $\mu\text{g mL}^{-1}$), and **4** (22.87% at a concentration of 100 $\mu\text{g mL}^{-1}$), respectively. The synthesized complexes failed to inhibit growth of the Gram-negative bacteria *P. putida* and the Gram-positive bacteria *B. cereus* at any concentration tested. These different inhibition results may be influenced by the particular bacteria under investigation as well as by differences in cellular penetration, distribution, metabolism, ejection from the cell, and possible off-target effects. Further mechanism studies are being undertaken and will be reported in due course.

4. Conclusion

In this study, we describe the synthesis and characterization of four copper(II) complexes supported by phenylacetic acid and diamine ligands. Their structures were determined by elemental analysis and single-crystal X-ray diffraction analysis. Each copper(II) adopts square-pyramidal geometry and all crystallize in the triclinic space group *P*-1. Their antimicrobial activities were evaluated against four different bacteria, and the results demonstrated that some of the complexes exhibit good antimicrobial activity. This work may stimulate an interest in further development of the novel copper(II) complexes as potentially useful antimicrobial agents.

Acknowledgements

This work was supported by Natural Science Foundation of Jiangsu Province [grant number BK20130554] and National Science & Technology Pillar Program during the Twelfth Five-year Plan Period [grant number 2012BAD36B01].

References

- [1] S.H. Eriksen, T. Bengt Söderblom, B. Jensen. *Biotechnol. Bioeng.*, **60**, 310 (1998).
- [2] J.G. Lee, B.Y. Lee, H.J. Lee. *Sci. Hort.*, **110**, 119 (2006).
- [3] D. Pizzeghello, A. Zanella, P. Carletti, S. Nardi. *Chemosphere*, **65**, 190 (2006).
- [4] K.D. Burkhead, P.J. Slininger, D.A. Schisler. *Soil Biol. Biochem.*, **30**, 665 (1998).
- [5] Y.-J. Zhu, H.-T. Zhou, Y.-H. Hu, J.-Y. Tang, M.-X. Su, Y.-J. Guo, Q.-X. Chen, B. Liu. *Food Chem.*, **124**, 298 (2011).
- [6] C. Cueva, M.V. Moreno-Arribas, P.J. Martín-Álvarez, G. Bills, M. Francisca Vicente, A. Basilio. *Res. Microbiol.*, **161**, 372 (2010).
- [7] C.W. Sheu, D. Salomon, J.L. Simmons, T. Sreevalsan. *Antimicrob. Agents Chemother.*, **7**, 349 (1975).
- [8] A. T'Ang, E.J. Lien. *J. Clin. Pharm. Ther.*, **6**, 45 (1981).
- [9] C. Braicu, A. Stanila, M.-A. Rotar, M. Petran, C. Socaciu. *Bull. USAMV Agric.*, **62**, 207 (2006).
- [10] G. Faúndez, M. Troncoso, P. Navarrete, G. Figueroa. *BMC Microbiol.*, **4**, 19 (2004).
- [11] J. Olsen, P. Seiler, B. Wagner, H. Fischer, T. Tschopp, U. Obst-Sander, D.W. Banner, M. Kansy, K. Müller, F. Diederich. *Org. Biomol. Chem.*, **2**, 1339 (2004).

- [12] C.Y. Kim, J.S. Chang, J.B. Doyon, T.T. Baird, C.A. Fierke, A. Jain, D.W. Christianson. *J. Am. Chem. Soc.*, **122**, 12125 (2000).
- [13] Z.H. Chohan, S.K.A. Sherazi. *Met.-Based Drugs*, **4**, 327 (1997).
- [14] M. Melník, M. Kabešová, M. Dunaj-Jurčo, C.E. Holloway. *J. Coord. Chem.*, **41**, 35 (1997).
- [15] A.W. Addison, T.N. Rao. *J. Chem. Soc., Dalton Trans.*, 1349 (1984).
- [16] S. Delgado, A. Muñoz, M.E. Medina. *Inorg. Chim. Acta*, **359**, 109 (2006).
- [17] D. Cremer, J.A. Pople. *J. Am. Chem. Soc.*, **97**, 1354 (1975).
- [18] Z.-M. Wang, B.-W. Sun, J. Luo, S. Gao, C.-S. Liao, C.-H. Yan, Y. Li. *Inorg. Chim. Acta*, **332**, 127 (2002).
- [19] A. Johansson, E. Wingstrand. *Inorg. Chim. Acta*, **358**, 3293 (2005).
- [20] M. Duggan, N. Ray, B. Hathaway, G. Tomlinson. *J. Chem. Soc., Dalton Trans.*, 1342 (1980).
- [21] M.R. Sundberg, R. Kivekäs, P. Huovilainen, R. Ugglä. *Inorg. Chim. Acta*, **324**, 212 (2001).
- [22] V.M. Nikitina, O.V. Nesterova, V.N. Kokozay, R.I. Zubatyuk, V.V. Dyakonenko, O.V. Shishkin, E.A. Goreshnik, C.J. Gómez-García. *Inorg. Chim. Acta*, **362**, 2237 (2009).
- [23] Y.X. Peng, F. Xu, G. Yin, Q. Liu, W. Huang. *J. Coord. Chem.*, **65**, 3949 (2012).
- [24] S. Mondal, M. Nayak, H. Sparkes, J. Howard, S. Mohanta. *J. Coord. Chem.*, **67**, 72 (2014).